BIOCHEMISTRY
including biophysical chemistry & molecular biology

Article

pubs.acs.org/biochemistry

Thermodynamic Signature of DNA Damage: Characterization of DNA with a 5-Hydroxy-2′-deoxycytidine·2′-Deoxyguanosine Base Pair

Manjori Ganguly,[†] Marta W. Szulik,[‡] Patrick S. Donahue,[‡] Kate Clancy,[†] Michael P. Stone,[‡] and Barry Gold*[,†]

[†]Department of Pharmaceutical Sciences, University of Pittsburgh, Pittsburgh, Pennsylvania 15261, United States
[‡]Department of Chemistry, Vanderbilt University, Nashville, Tennessee 37235, United States

ABSTRACT: Oxidation of DNA due to exposure to reactive oxygen species is a major source of DNA damage. One of the oxidation lesions formed, 5-hydroxy-2′-deoxycytidine, has been shown to miscode by some replicative DNA polymerases but not by error prone polymerases capable of translesion synthesis. The 5-hydroxy-2′-deoxycytidine lesion is repaired by DNA glycosylases that require the 5-hydroxycytidine base to be extrahelical so it can enter into the enzyme's active site where it is excised off the DNA backbone to afford an abasic site. The thermodynamic and nuclear magnetic resonance results presented here describe the effect of a 5-hydroxy-2′-deoxycytidine·2′-deoxyguanosine base pair on the stability of two different DNA duplexes. The results demonstrate that the lesion is highly destabilizing and that the energy barrier for the unstacking of 5-hydroxy-2′-deoxycytidine from the DNA duplex may be low. This could provide a thermodynamic mode of adduct identification by DNA glycosylases that requires the lesion to be extrahelical.

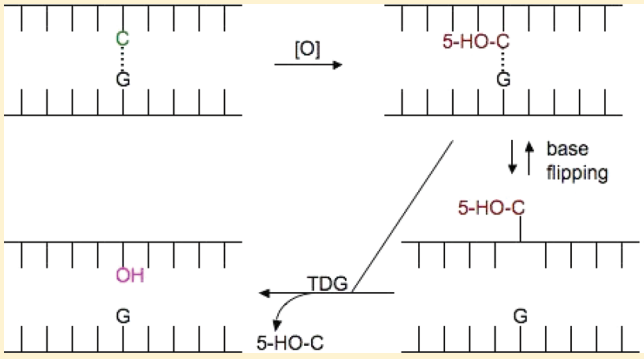

The inadvertent oxidation of DNA is one of the most common types of DNA damage that occurs in cells, with thousands of oxidized DNA base lesions formed per cell per day.[1−7] The most common oxidative modification is 8-oxoguanine (oxoG), which can interfere with DNA replication and cause an increase in the number of mutations.[8−17] Other sites of attack are at adenine and cytosine. In the case of the latter, 2′-deoxycytidine (dC) can be transformed into 5-hydroxy-2′-deoxycytidine (HO-dC) by a one-electron oxidation and subsequent attack by water on the intermediate radical cation, or via dehydration of 5,6-dihydroxy-2′-deoxycytidine, another oxidation product that forms in cells.[18−20] In turn, HO-dC can afford 5-hydroxy-2′-deoxyuridine (HO-dU) via deamination.

In vitro replication of DNA with a HO-dC residue in the template strand is prone to errors based upon the sequence context,[21] so the modified base represents a potential promutagenic lesion. Other studies in *Escherichia coli* and *Saccharomyces cerevisiae* imply that a single-stranded template with a HO-dC lesion is read correctly; i.e., it encodes dG.[22,23] It has also been reported that the error prone polymerase Polι bypasses HO-dC without miscoding.[24] In most studies, the deamination product, HO-dU, is dominant in terms of toxicity and mutagenicity derived from the initial formation of HO-dC.[21−23]

Recently, the crystal structure of HO-dC in DNA has been reported in the context of the structural impact of the lesion on DNA polymerization by the bacteriophage RB69 polymerase.[25] The study shows that HO-dC in the template strand can stabilize the incoming dGMP via canonical Watson−Crick base pairing, while incorporation of dAMP opposite the lesion leads to destabilizing unstacking. Similar to what has previously been reported, the misincorporation of dAMP opposite HO-dC occurs at a rate 5 times that for dC.

Because the repair of HO-dC by different DNA repair glycosylase proteins requires the lesion to rotate out of the double helix and into the enzyme's active site,[26−30] we initiated an investigation of the thermodynamic effects of HO-dC on DNA stability with a specific interest in whether it remains stably stacked in the double helix. We were also interested in seeing how the presence of a polar hydroxyl group in the major groove would affect the hydration of DNA and the association of cations. Both play an important role in the enthalpic stabilization of duplex DNA. The thermodynamic and nuclear magnetic resonance (NMR) results show a remarkable destabilizing effect for the HO-dC·dG base pair and that it may readily adopt an extrahelical conformation, which may facilitate its initial recognition by DNA repair proteins. This endothermic change in free energy due to the HO-dC modification is accompanied by a large reduction in the level of release of cations and structural water from the DNA upon unfolding.

Received: January 9, 2012
Revised: February 13, 2012
Published: February 14, 2012

   dx.doi.org/10.1021/bi3000269 | *Biochemistry* 2012, 51, 2018−2027

MATERIALS AND METHODS

Materials. The oligodeoxynucleotides were synthesized and purified via high-performance liquid chromatography (HPLC) by Invitrogen (Frederick, MD). The samples were desalted by gel-permeation chromatography, using a Sephadex G-25 column, lyophilized to dryness, and characterized by matrix-assisted laser desorption ionization time-of-flight mass spectometry (MALDI-TOF MS). We annealed the dry oligomers by dissolving the single-stranded oligodeoxynucleotides in appropriate buffer, heating the solution to 90 °C for 10 min, and allowing it to cool slowly to room temperature.

The concentration of the oligomer solutions was determined at 260 nm and 80 °C using an extinction coefficient of ~1.11×10^5 M^{-1} cm^{-1} (ODNs **1**−**4**) and 1.08×10^5 M^{-1} cm^{-1} (ODN **5**) at 260 nm and 25 °C assuming similar extinction coefficients for 5-OH-dC and dC. This value was obtained from the molar absorptivity at 25 °C, obtained from the tabulated values of the dimers and monomer bases,[31] and extrapolated to high temperatures using the upper portions of the UV melting curves, following procedures described previously.[32] Stock solutions at different pH values were prepared from 100 mM sodium phosphate buffer (100 mM mono- and dibasic forms) adjusted to the appropriate pH using either mono- or dibasic sodium phosphate solutions and diluted to 10 mM when required. Na^+ and osmolyte concentrations were adjusted using a NaCl solution and ethylene glycol, respectively. All solutions were filtered through a 0.20 μm filter (Alltech Associates, Inc.) and degassed before being used.

Temperature-Dependent UV Spectroscopy. Absorption versus temperature profiles (UV melts) for each duplex were measured at either 260 or 275 nm using a Varian (Palo Alto, CA) Cary 300 spectrophotometer equipped with a Peltier temperature controller and interfaced with a computer for data acquisition and analysis. The temperature was scanned at heating rates of 1.00 °C/min. Melting curves as a function of strand concentration (4−50 μM) were obtained to check for the molecularity of each molecule. Additional melting curves were obtained as a function of pH, salt concentration, and osmolyte concentration to determine the differential binding of counterions and water molecules that accompanies their helix → coil transitions.

UV melts were measured in the salt range of 10−200 mM NaCl at neutral pH, and at a constant total strand concentration of 5 μM, to determine the differential binding of counterions, Δn_{Na^+}, which accompanied their helix−coil melting. This linking number was measured experimentally with the assumption that binding of counterions to the helical and coil states of each oligonucleotide took place with a similar type of binding using the relationship[33]

$$\Delta n_{Na^+} = (\Delta H_{cal}/RT_M^2)(\partial T_M/\partial \ln[Na^+]) \quad (1)$$

The numerical factor corresponded to the conversion of ionic activities into concentrations. The first term in parentheses ($\Delta H_{cal}/RT_M^2$) was a constant determined directly from DSC experiments, where R is the gas constant. The second term in parentheses was determined from UV experiments from the dependencies of T_M on salt concentration.

For the determination of Δn_w, UV melts were measured in the ethylene glycol concentration range of 0.5−3.0 m at pH 7.0 and 10 mM NaCl and at a constant total strand concentration of 5.0 μM. The osmolalities of the solutions were obtained with a Wescor (Logan, UT) model 5520 Vapro vapor pressure osmometer. These osmolalities were then converted into water activities, a_w, using the equation[34]

$$\ln(a_w) = -(\mathrm{Osm}/M_w) \quad (2)$$

where Osm is the solution osmolality and M_w is the molality of pure H_2O, equal to 55.5 mol/kg of H_2O. Differential binding of water, Δn_w, was calculated using the relationship[33]

$$\Delta n_w = (\Delta H_{cal}/RT_M^2)(\partial T_M/\partial \ln a_W) \quad (3)$$

The $\Delta H_{cal}/RT_M^2$ term used in the determination of Δn_w at higher salt concentrations is the one obtained experimentally at the particular salt concentration.

Differential Scanning Calorimetry. All calorimetric experiments were conducted using a VP-DSC differential scanning calorimeter (Microcal, Inc., Northampton, MA). The dry oligodeoxynucleotides were dissolved in 10 mM sodium phosphate buffer (pH 7.0) and adjusted to the desired ionic strength with NaCl for all unfolding experiments. In a typical DSC experiment, ~0.75 mL of a dilute aqueous solution of oligonucleotide (125−200 μM) was loaded into a sample cell and a matched reference buffer solution loaded into a reference cell. Each solution was thermally scanned from 0 to 100 °C at a constant heating rate of 45 °C/h over five forward scans. The DSC melting curves were normalized by the heating rate, and a buffer versus buffer scan was subtracted and normalized for the number of moles. The resulting curves were then analyzed with Origin version 7.0 (Microcal, Inc.); their integration ($\int \Delta C_p\, dT$) yielded the molar unfolding enthalpy (ΔH_{cal}), which was independent of the nature of the transition.[35,36] The molar entropy (ΔS_{cal}) was obtained similarly, using $\int (\Delta C_p/T)\, dT$. The Gibbs free energy change at any temperature T was then obtained with the Gibbs equation $\Delta G°(T) = \Delta H_{cal} - T\Delta S_{cal}$.

Circular Dichroism. Circular dichroism (CD) spectra were recorded on a Jasco (Easton, MD) model J-815 CD spectrometer equipped with a Peltier device and nitrogen purging capabilities. The spectrum of each duplex was obtained using a strain-free 1 cm quartz cell at low temperatures to ensure 100% duplex formation. Data were collected at 4 and 90 °C. Typically, 1 OD unit of a duplex sample was dissolved in 1 mL of a buffer containing 10 mM sodium phosphate (pH 7.0). After equilibration for 5 min at each sample temperature, the instrument collected spectral data in the 220−350 nm range every 1.0 nm.

NMR Studies. Samples for the observation of exchangeable protons were dissolved to a duplex concentration of 81 nM in 180 μL of 10 mM NaH_2PO_4, 100 mM NaCl, and 50 μM Na_2EDTA buffer (pH 7.0) containing a 9:1 (v/v) H_2O/D_2O mixture. One- and two-dimensional (1D and 2D, respectively) NMR experiments were performed on a Bruker Avance spectrometer operating at 900 MHz. Chemical shifts were referenced to the water resonance. NMR data were processed using TOPSPIN version 3.0 (Bruker Inc., Karlsruhe, Germany). 1D NMR spectra for the exchangeable protons were recorded at 5, 15, 25, 35, 45, 55, and 60 °C. The $^1H-^1H$ NOESY spectra of unmodified and modified samples in H_2O were recorded at 5 °C, with mixing times of 70 and 250 ms and a relaxation delay of 2.0 s. These experiments were conducted using a field gradient Watergate pulse sequence for water suppression.

RESULTS

The HO-dC lesion, which is commercially available as the protected phosphoramidite, was incorporated into two different

dx.doi.org/10.1021/bi3000269 | Biochemistry 2012, 51, 2018−2027

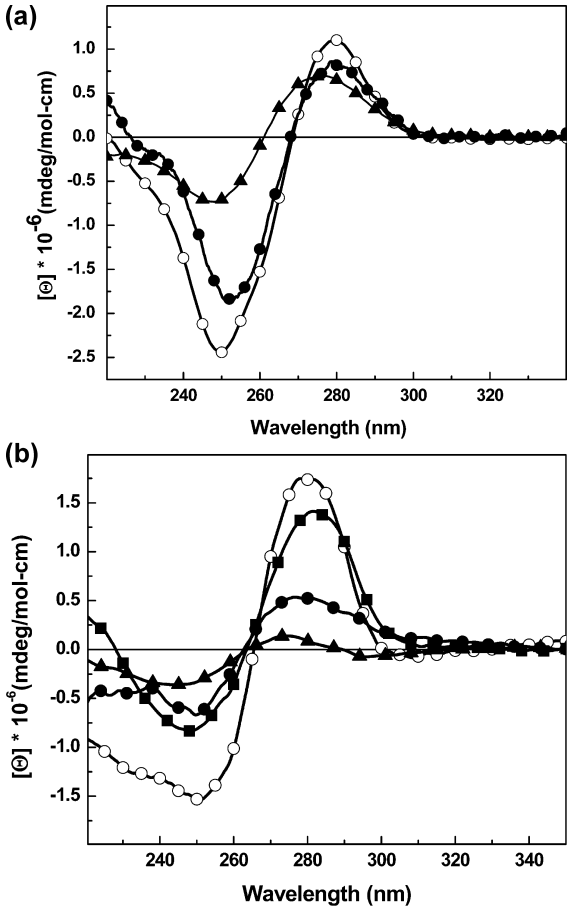

Figure 1. CD spectra of (a) ODN **1** (○), ODN **2** (●), and ODN **1** (▲) heated to 90 °C and (b) ODN **3** (○), ODN **4** (●), ODN **5** (■), and ODN **3** (▲) heated to 90 °C.

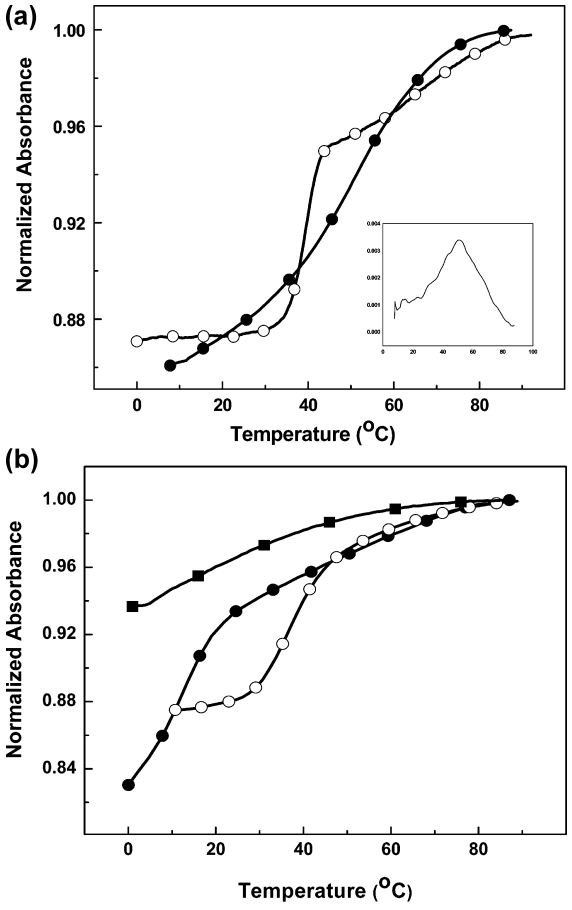

Figure 2. (a) UV melting curves of ODN **1** (●) and ODN **2** (○) and (b) ODN **3** (○), ODN **4** (●), and ODN **5** (■) in 10 mM sodium phosphate buffer (pH 7.0) at a strand concentration of ~10 μM.

self-complementary oligodeoxynucleotide (ODN) sequences (Table 1). All ODNs were purified by HPLC and analyzed by MALDI-TOF to demonstrate their purity and identity. ODN **1** and **2** are based on the well-studied Drew Dickerson dodecamer[37] that has G/C rich termini and an A/T rich central core. ODN **3** and **4** lack the A/T central core, which minimizes the formation of hairpin structures that tend to form in solutions of ODN **1** under certain conditions.[38]

CD. To confirm that the global conformation of the HO-dC-modified DNAs, the CD spectrum of ODN **2** was obtained and compared to that of control ODN **1** (Figure 1a). Both duplexes show an overall normal B-DNA conformation, but there is a modest reduction in the intensity of the negative band near 250 nm in ODN **2** that is indicative of weakened base stacking.[39] A similar result is seen with ODN **4** versus ODN **3** (Figure 1b). For the purposes of comparison, we synthesized an analogous self-complementary DNA sequence (ODN **5**) with a dC·dC mismatch in place of the HO-dC·dG pair and determined its CD spectrum at low temperatures (Figure 1b). The intensities of the positive and negative bands fall midway between those of the unmodified DNA and the DNA with the HO-dC·dG base pair.

Table 1. Standard Thermodynamic Profiles[a] for 5-HO-dC (X)-Modified DNA at pH 7.0 in 10 mM Sodium Phosphate Buffer

ODN	sequence	[NaCl] (mM)	T_M (°C)	ΔH (kcal/mol)	$\Delta G°$ (kcal/mol)	$T\Delta S$ (kcal/mol)	Δn_{Na^+} (no. of waters/mol of DNA)	Δn_w (no. of waters/mol of DNA)
1	CGCGAATTCGCG GCGCTTAAGCGC	10	33.3	−116.0	−6.9	−109.0	−2.3 ± 0.15	−38.0 ± 2.0
2	CGCGAATTXGCG GCGXTTAAGCGC	10	31.5	−74.3	−2.8	−71.5	−1.0 ± 0.11	−21.0 ± 3.0
3	GAGAGCGCTCTC CTCTCGCGAGAG	10	41.3	−78.2	−6.9	−71.3	−3.4 ± 0.2	−41.0 ± 3.0
4	GAGAGCGCTXTC CTXTCGCGAGAG	10	15.0	−41.7	−0.7	−41.0	−2.3 ± 0.15	−13.0 ± 1.0
5	GACAGCGCTCTC CTCTCGCGACAG	10	8.5	−31.1	0.2	−31.3	nd[b]	nd[b]

[a]Oligomer concentration of 10 μM. [b]Not determined.

dx.doi.org/10.1021/bi3000269 | *Biochemistry* 2012, 51, 2018−2027

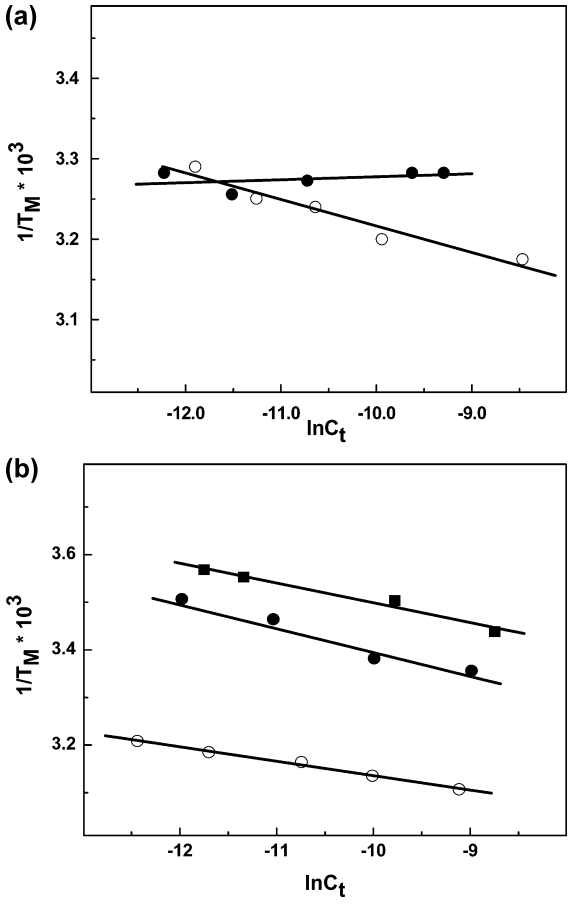

Figure 3. (a) Dependence of T_M on strand concentration of ODN **1** (○) and ODN **2** (●) and (b) ODN **3** (○), ODN **4** (●), and ODN **5** (■) in 10 mM sodium phosphate buffer (pH 7.0) at strand concentrations of ~4−75 μM.

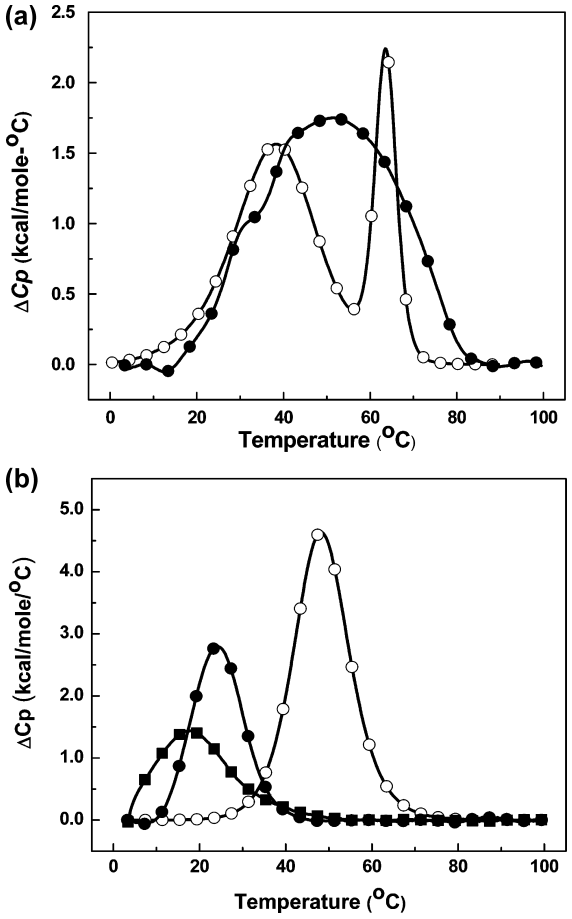

Figure 4. Differential scanning calorimetry (DSC) curves in 10 mM sodium phosphate buffer (pH 7.0) (a) at strand concentrations of ~150−200 μM for (a) ODN **1** (○) and ODN **2** (●) and (b) at strand concentrations of ~124−150 μM for ODN **3** (○), ODN **4** (●), and ODN **5** (■).

Thermodynamic Characterization of DNA with HO-dC Lesions. The thermal melts of the five duplexes were followed by monitoring the absorbance at 260 nm as a function of temperature. ODN **1** shows what appears to be a classical two-state unfolding (Figure 2a) with a T_M of 33.3 °C (Table 1). The unfolding of ODN **2** occurs with a broad transition, and there appear to be multiple transitions (Figure 2a). Because of this result, we looked at the effect of strand concentration to determine whether ODN **2** was forming a hairpin (Figure 3a). As expected, ODN **1** showed a dependence of T_M on strand concentration, but HO-dC-modified ODN **2** did not. The linear response of ODN **2** suggests that it is preferentially forming a unimolecular hairpin. This would explain the broad melt in Figure 2a due to the presence of a mixture of duplex and hairpin structures even at the lower temperatures. ODN **3**, ODN **4**, and ODN **5** showed a dependence of T_M on strand concentration (Figure 3b). DSC analyses of ODNs **1** and **2** at low salt concentrations are also consistent with the latter having multiple folded structures with different melting transitions (Figure 4a). In contrast, ODN **1** shows a well-resolved melt indicating the presence of the duplex (the low-temperature transition) and hairpin (the high-temperature transition). Clearly, the presence of the HO-dC has a significant destabilizing effect on the central domain of the duplex form of ODN **2**.

To avoid the complication associated with intramolecular hairpin formation, we turned to the analysis of ODNs **3** and **4**. ODN **3** does not form a hairpin because of the G/C rich central core. The UV melts for this pair of duplexes are shown in Figure 4a and reveal a dramatic reduction in the T_M due to HO-dC ($\Delta\Delta T_M$ is ~24 °C at high concentrations). Even at 0 °C, the UV melt of ODN **4** does not afford a linear baseline. It is also apparent that the hyperchromicity, which reflects changes in base stacking, is significantly reduced in ODN **4** versus that in ODN **3**. The DSC plots of ODNs **3** and **4** (Figure 4b) corroborate the difference in stability observed in the UV melting experiment and provide quantification of the difference in $\Delta\Delta G°$, which is more than 6 kcal/mol (Table 1). The DSC plots show that both ODNs **3** and **4** unfold in single sharp transitions. The loss of stabilization is mainly due to the 36 kcal/mol reduction in the stabilizing enthalpy term that is not fully compensated by the increase in entropy (Table 1).

The UV melt and DSC of the DNA with the dC·dC mismatch (ODN **5**) provide a comparison to ODN. The UV melt of ODN **5** shows a broad transition (T_M ~ 8 °C) with little hyperchromicity (Figure 2b). The DSC thermogram of ODN **5** has a similar pattern with a broad low-temperature curve with a $\Delta\Delta G°$ of ~7 kcal/mol relative to ODN **3** (Table 1) because of an endothermic $\Delta\Delta H$ of 47 kcal/mol.

NMR Studies. To determine how the HO-dC residue affected base pairing within the DNA sequence, the imino proton resonances of ODNs **1** and **2** were assigned. Figure 5

dx.doi.org/10.1021/bi3000269 | *Biochemistry* 2012, 51, 2018−2027

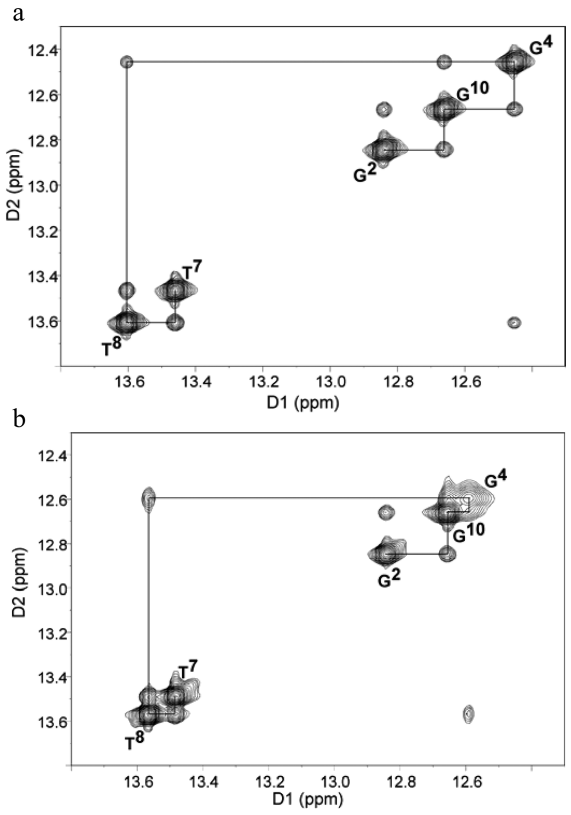

Figure 5. $^{1}H-^{1}H$ NMR NOESY spectrum showing resonances for the thymine and guanine imino protons and sequential NOE connectivity for the imino protons of the $G^{2}\cdot C^{11}$ to $A^{6}\cdot T^{7}$ base pairs for (a) unmodified ODN **1** and (b) 5-HO-dC-modified ODN **2**.

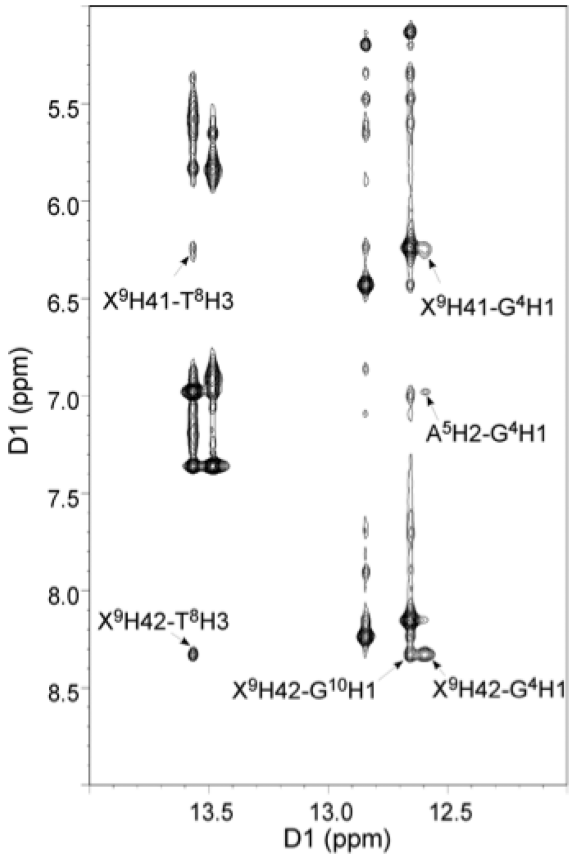

Figure 6. Expansion of the $^{1}H-^{1}H$ NOESY spectrum for 5-OH-dC-modified ODN **2**, showing the conservation of Watson–Crick base pairing and base stacking.

shows the NOE connectivity of the purine N1 and pyrimidine N3 imino protons. The imino protons were assigned on the basis of their sequential connectivities in NOESY spectra, and these assignments were supported by their NOE cross-peaks to Watson–Crick base-paired amino protons.[40] The sequential connectivities were obtained from base pairs $G^{2}\cdot C^{11} \rightarrow G^{10}\cdot C^{3} \rightarrow G^{4}\cdot X^{9}/C^{9} \rightarrow T^{8}\cdot A^{5} \rightarrow T^{7}\cdot A^{6}$. For both duplexes, the imino proton resonances of the terminal $C^{1}\cdot G^{12}$ base pairs are lost through fast exchange with water. The imino resonance from G^{4}, which is base paired with X^{9}, was less intense and broader compared to that from G^{4} for the unmodified duplex. Moreover, the G^{4} imino peak was shifted downfield (by 0.15 ppm), which reflected the effect of base pairing with the opposing X^{9}. Figure 6 shows the region of the NOESY spectrum showing the NOEs between the imino and amino protons. The G^{4} H1 imino proton appeared as a broad peak at 12.6 ppm (Figure 5b); it exhibited weak cross-peaks with X^{9}-N^{4} H1, X^{9}-N^{4} H1, and A^{5} H2. In addition, X^{9} amino protons with T^{8} H3 cross-peaks were also observable.

A series of 1D NMR spectra for the exchangeable protons of ODNs **1** and **2** were recorded at 5, 15, 25, 35, 45, 55, and 60 °C (Figure 7a). The temperature dependencies of the line widths for base pairs of unmodified and modified duplexes are compared in Figure 7b. The N^{1}-imino proton of the $X^{9}\cdot G^{4}$ modified base pair in ODN **2** was already broad at 5 °C and disappeared at higher temperatures. In unmodified ODN **1**, the same imino proton resonance remained sharp even at temperatures as high as 45–50 °C. The NMR data also show that the N^{1}-imino proton of the $G^{2}\cdot C^{11}$ base pair in modified ODN **2** was sharp only at 5 °C; when the temperature was increased, the peak started to broaden and finally disappeared at 25 °C. In unmodified ODN **1**, the $G^{2}\cdot C^{11}$ imino proton was sharp up to room temperature, above which it started to become broader. The $G^{10}\cdot C^{3}$ base pair, which is adjacent to the $X^{9}\cdot G^{4}$ pair, could almost not be observed at 35 °C in ODN **2**, while it is still sharp even at 45 °C for ODN **1**. The peak corresponding to T^{8}, which is immediately adjacent to the $X^{9}\cdot G^{4}$ pair in ODN **2**, started to broaden at approximately 35 °C, while the same imino proton in ODN **1** was still visible at 55 °C. The imino resonance of the $T^{7}\cdot A^{6}$ base pair remained sharp for ODN **2** and disappeared above 45 °C; however, for ODN **1**, the same imino proton remained sharp and intense at this temperature.

The temperature-dependent NMR data show increased rates of exchange among the $G^{4}\cdot X^{9}$, $G^{2}\cdot C^{11}$, and $G^{10}\cdot C^{3}$ base pairs and solvent, which suggest that base pairing is destabilized compared to that of unmodified duplex ODN **1**. In addition, the expanded NOESY spectrum showed a broad cross-peak between modified X^{9} and the complementary G^{4}, indicating weaker Watson–Crick base pairing in comparison to that of the unmodified duplex. The presence of the cross-peaks between amino X^{9} and imino G^{10} and T^{8} suggests conserved base stacking of OH-dC with neighboring bases. However, this interaction appears as a set of broad cross-peaks that implies weaker interaction than for other peaks but also reflects structural changes, which are still under investigation.

Effect of HO-dC on DNA Hydration and Cation Binding. To understand the origin of the destabilization observed in the DSC and NMR experiments, we probed the

dx.doi.org/10.1021/bi3000269 | *Biochemistry* 2012, 51, 2018–2027

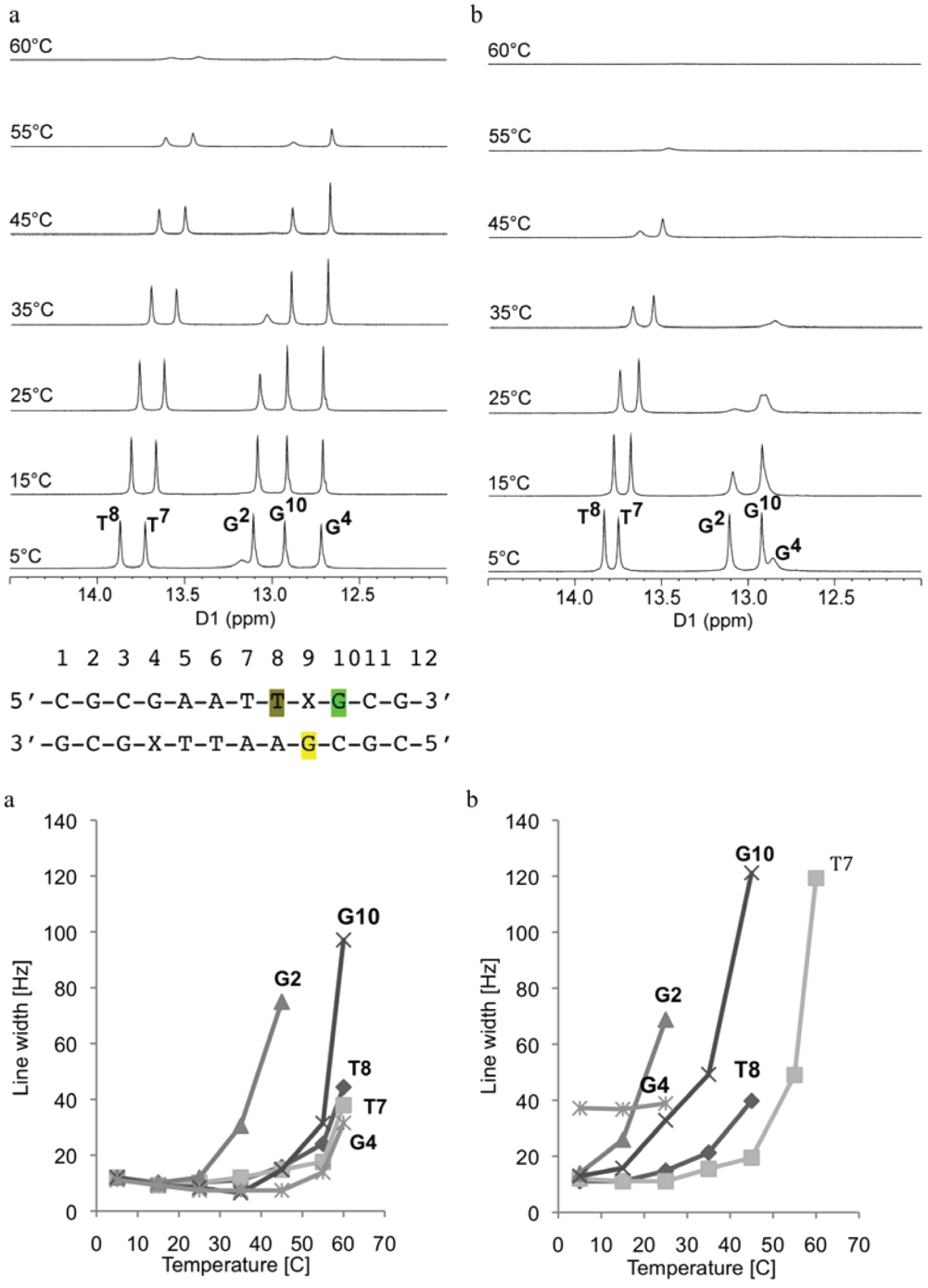

Figure 7. ^{1}H NMR spectra of imino proton resonances as a function of temperature for (a) unmodified ODN **1** and (b) 5-HO-dC-modified ODN **2** (top). Temperature dependence of line widths of the imino proton resonances of (a) unmodified ODN **1** and (b) 5-HO-dC-modified ODN **2** (bottom).

effect of the HO-dC lesion on the binding of water and cations to ODN **2** versus ODN **1** and ODN **4** versus ODN **3** (Figures 8 and 9, respectively). The $\Delta\Delta n_W$ for ODN **2** relative to ODN **1** is 17 waters/mol of DNA, while the change is even greater for ODN **4** relative to ODN **3** ($\Delta\Delta n_W$ = 28 waters/mol) (Table 1). There was also a significant reduction in the level of release of cations from the modified duplexes: $\Delta\Delta n_{Na^+}$ values of 1.3 and 1.1 Na^+/mol of DNA for ODN **1** versus ODN **2** and ODN **3** versus ODN **4**, respectively. These changes are consistent with a reduction in the level of base pair stacking; double-stranded DNA is more hydrated and has more cations associated with it than single-strand DNA despite the larger number of polar heteroatoms that are accessible in single-stranded DNA.[41,42]

DISCUSSION

Why is the HO-dC·dG base pair in DNA so unstable? To check the stability of the HO-dC-modified oligomers, we re-ran the MALDI-TOF MS of ODN **4** after the thermodynamic studies were completed, and it showed the same spectrum as it did when we initially purified it; therefore, chemical degradation of the lesion cannot account for the NMR and thermodynamic

dx.doi.org/10.1021/bi3000269 | *Biochemistry* 2012, 51, 2018−2027

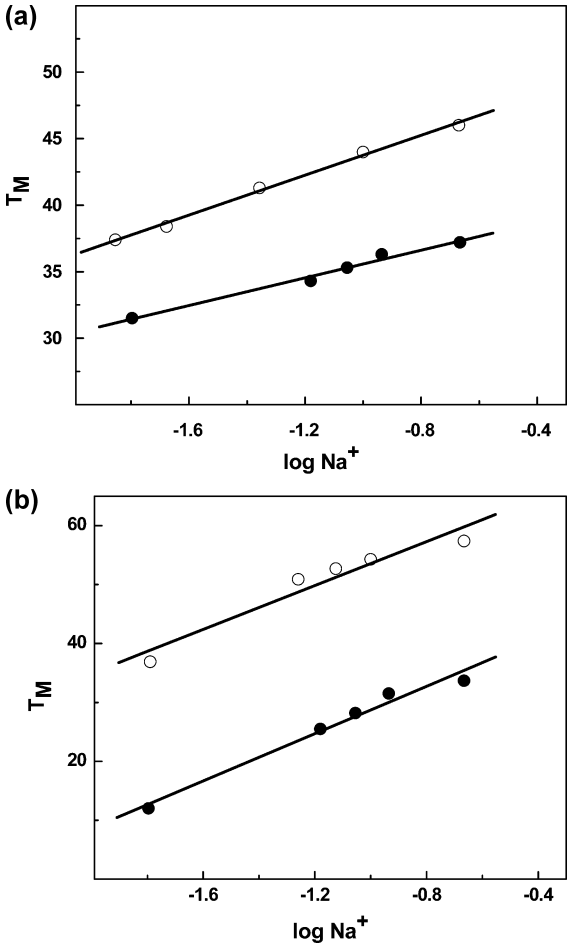

Figure 8. (a) Dependence of T_M on salt concentration for ODN **1** (○) and ODN **2** (●) in 10 mM sodium phosphate buffer (pH 7.0) and (b) ODN **3** (○) and ODN **4** (●) at a strand concentration of ∼8 μM.

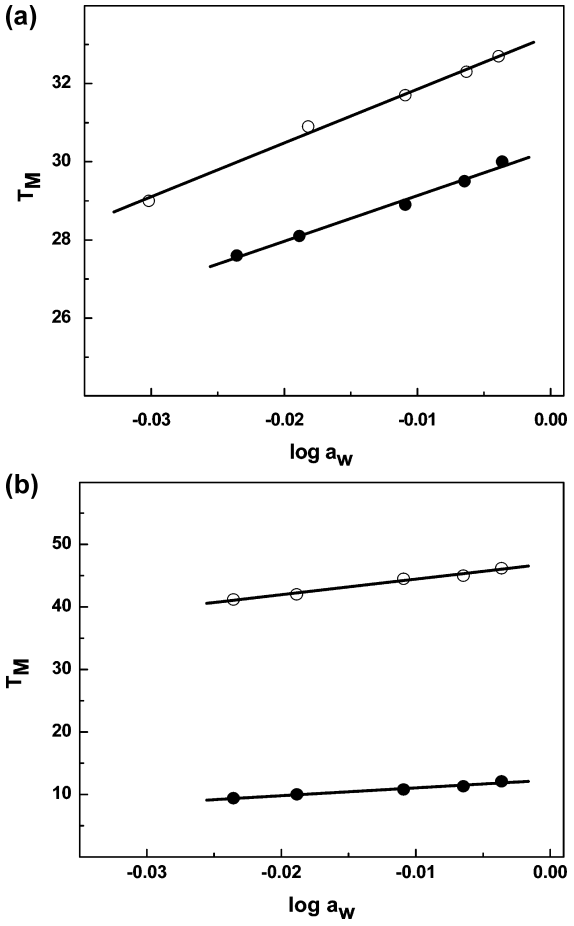

Figure 9. (a) Dependence of T_M on osmolyte concentration (function of ethylene glycol) for ODN **1** (○) and ODN **2** (●) and (b) ODN **3** (○) and ODN **4** (●) in 10 mM sodium phosphate buffer (pH 7.0) at a strand concentration of ∼8 μM.

observations. The equilibrium between the amino and imino tautomeric forms for the deoxynucleoside has been studied by NMR[43] and UV resonance Raman spectroscopy.[44] In the former, there was no change in the preference for the "normal" amino tautomer within the detection limits of the method when the pH was adjusted so the nucleoside was in the neutral form. In the Raman study, a 100-fold increase in the level of the imino tautomer was reported, but it still comprised less than 0.1% of the predominant amino tautomer. The increase in the level of the rare imino tautomer could be in part responsible for the infrequent G → A transitional mutations that arise from this lesion during DNA replication, but it cannot explain the dramatic effect in the thermodynamic or NMR measurements. Moreover, the structure of HO-dC in the primer strand paired with a 3′-dGMP within the active site of a DNA polymerase adopts a classical Watson−Crick alignment with no evidence of a wobble pair arrangement in the crystal structure.[25]

In the nonionized (neutral) form, the 5-hydroxy group of HO-dC can move within 3.7 Å of the 5′-nonbridging phosphate oxygen that points into the major groove in a canonical B-DNA conformation. This type of H-bond interaction could generate a locally distorted base pairing structure. The 5-hydroxyl group on HO-dC can ionize near neutral pH: the pK_a for this process was calculated to be 7.3 for the nucleoside and 8.5 for the nucleotide.[45] The ionization of the 5-hydroxy group could locally destabilize the DNA because of a repulsive electrostatic interaction between the ionized $^-$O-dC (i.e., anionic) and the polyanionic phosphodiester backbone. To explore this possibility, we ran UV melts of ODNs **3** and **4** at pH values that bracketed the reported pK_a of HO-dC. We observed that the ΔT_M between ODNs **3** and **4** at the different pH values remained fairly constant, although both unmodified and modified duplexes were marginally less stable under the more acidic conditions (Table 2). There was also little change in the hyperchromicity observed in the melts, suggesting a minimal pH-dependent change in base stacking. There are several potential explanations for this result. The pK_a of HO-dC in a double helix may be significantly altered because of reduced water activity in the major groove.[46] This has been observed for the pK_a of dC where protonation of the N3 position is required for the formation of stable C^+-G·C triplets.[47,48] The pK_a of dC is ∼4.3,[49] while in an intermolecular triplex, it can be as high as 6 and as high as 7 in an intramolecular triplex.[50] If this is the case for the 5-hydroxyl group, the pH range used in our stability studies may not have captured the ionized form.

An alternative explanation for the effect of HO-dC is the effect of the 5-hydroxy group on the magnitude of the base's dipole moment. Multiconfiguration self-consistent field (MCSCF) calculations indicate that there is a dramatic decrease in the dipole moment for the amino−keto tautomer of HO-dC (4.61[51] or 4.8−5.9 D[52] versus 6.08−7.61 D for

dx.doi.org/10.1021/bi3000269 | *Biochemistry* 2012, 51, 2018−2027

Table 2. Effect of pH on the T_M and Hyperchromicity of Unmodified DNA and 5-HO-dC (X)-Substituted DNA at 100 mM NaCl in 10 mM Sodium Phosphate Buffer

pH	GAGAGCGCTCTC T_M (°C)	hyperchromicity (%)	GAGAGCGCTXTC T_M (°C)	hyperchromicity (%)
5.5	52.7	13.4	22.1	11.9
6.4	55.1	12.5	27.4	9.2
7.0	55.3	12.9	28.2	10.2
8.5	54.7	14.1	25.8	13.3

dC[53]), which will electrostatically destabilize the pairing with the strong antiparallel dipole moment of dG.

The magnitude of the destabilization suggested that the HO-dC·dG may not be forming a base pair in solution via a three-H-bond Watson−Crick motif despite the canonical crystal structure of HO-dC with dGMP at the active site of bacteriophage DNA polymerase.[25] A duplex was prepared with a dC·dC mismatch to see how it compared to ODN **4**. The dC·dC mismatch, which is generally the most destabilizing base pair arrangement,[54] does not form a hairpin (Figure 4b) and is even more destabilizing than the HO-dC·dG mismatch (Table 1). The CD of mismatched ODN **5** is actually more similar to that of ODN **3** than to that of ODN **4**. However, the $\Delta\Delta G°$ and ΔT_M between ODN **4** and ODN **5** from the thermodynamic studies indicate that the pairing between HO-dC and dG behaves like a dC·dC mismatch that can form only one H-bond assuming the predominance of the neutral amino tautomer.

While the destabilization induced by the HO-dC·dG pair is pronounced, we have reported similar thermodynamic parameters for other oxidized bases and for alkylated lesions. For example, an 8-oxo-dG·dC base pair causes a significant destabilization ($\Delta\Delta G$ > 3 kcal/mol) that is driven by a >35 kcal/mol reduction in the ΔH term.[55] As seen with the HO-dC·dG-modified DNA, the effect can be observed by temperature-dependent monitoring of the imino proton resonances, and there is a concomitant reduction in the release of water and cations upon the unfolding of the DNA with the oxidized lesion. Despite these thermodynamic differences, the crystal[56] and high-resolution NMR[57] structures of DNA with 8-oxo-dG·dC are indistinguishable from those of wild-type DNA. As is often the case, the similarity in structures for unmodified and 8-oxoguanine-modified DNA by these two structural techniques does imply that the molecules will have similar thermal or thermodynamic characteristics. They clearly do not.

The pattern is the same for DNA with 3-methyl-3-deaza-dA·dT,[58] 3-deaza-dA·dT,[58] 7-deaza-dG·dC,[59] and 7-deaza-dA·dT[60] base pairs. In all cases, we observed reduced stability because of an unfavorable enthalpic change that is not fully offset by the increase in the entropy term. Moreover, these modified duplexes are characterized by a reduced level of release of hydrophobic water and cations upon unfolding.

We propose that the local destabilization of DNA affords a thermodynamic signature that can be exploited by base excision repair glycosylases in the initial screening of the genome for lesions, a suggestion originally made by Plum and Breslauer.[61] While the lesions may not extensively populate an extrahelical conformation, the energetic penalty required to extrude them from the base stack and deform the DNA backbone[62] will be significantly reduced. It is known that glycosylase binding is accelerated when the lesion is in a mismatch.[63,64] Thus, as the glycosylases "scan" the DNA, the low energy barrier for forming a DNA conformation that initially stabilizes the interaction of the protein with the DNA would constitute a thermodynamically based mechanism of lesion detection. If the lesion is a substrate for the glycosylase, it will be excised off the backbone. If not, the complex will collapse and the glycosylase can continue to scan the DNA for lesions. A related proposal is the explanation for the specificity of the alkyladenine DNA glycosylase for substrate lesions derived from a detailed study of the kinetics of base flipping and excision of 1,N6-ethenoadenine by alkyladenine DNA glycosylase.[65] Related to this suggestion of specificity being based on the ease of base extrusion is the report that the bacterial AlkD glycosylase catalyzes the hydrolysis of N3-methyladenine off the DNA backbone by stabilizing it as an extrahelical lesion.[66] In this case, no enzymatic step is required because the rate of hydrolysis of 3-methyladenine from the deoxyribose in single-stranded DNA is quite rapid even at neutral pH.[67]

AUTHOR INFORMATION

Corresponding Author

*E-mail: goldbi@pitt.edu. Telephone: (412) 383-9593.

Funding

This work was supported in part by the National Cancer Institute Grant CA29088.

Notes

The authors declare no competing financial interest.

REFERENCES

(1) Wagner, J. R., Hu, C. C., and Ames, B. N. (1992) Endogenous oxidative damage of deoxycytidine in DNA. *Proc. Natl. Acad. Sci. U.S.A. 89*, 3380−3384.

(2) Imlay, J. A., and Linn, S. (1988) DNA damage and oxygen radical toxicity. *Science 240*, 1302−1309.

(3) O'Brien, P. J. (1988) Radical formation during the peroxidase catalyzed metabolism of carcinogens and xenobiotics: The reactivity of these radicals with GSH, DNA, and unsaturated lipid. *Free Radical Biol. Med. 4*, 169−183.

(4) von Sonntag, C. (1991) The chemistry of free-radical-mediated DNA damage. *Basic Life Sci. 58*, 287−317.

(5) Dizdaroglu, M. (1991) Chemical determination of free radical-induced damage to DNA. *Free Radical Biol. Med. 10*, 225−242.

(6) Halliwell, B., and Gutteridge, J. M. (1992) Biologically relevant metal ion-dependent hydroxyl radical generation. An update. *FEBS Lett. 307*, 108−112.

(7) Dizdaroglu, M. (1992) Oxidative damage to DNA in mammalian chromatin. *Mutat. Res. 275*, 331−342.

(8) Floyd, R. A. (1990) The role of 8-hydroxyguanine in carcinogenesis. *Carcinogenesis 11*, 1447−1450.

(9) Dizdaroglu, M. (1985) Formation of an 8-hydroxyguanine moiety in deoxyribonucleic acid on γ-irradiation in aqueous solution. *Biochemistry 24*, 4476−4481.

(10) Kasai, H., and Nishimura, S. (1986) Hydroxylation of guanine in nucleosides and DNA at the C-8 position by heated glucose and oxygen radical-forming agents. *Environ. Health Perspect. 67*, 111−116.

(11) Kasai, H., Crain, P. F., Kuchino, Y., Nishimura, S., Ootsuyama, A., and Tanooka, H. (1986) *Carcinogenesis 7*, 1849−1851.

(12) Abu-Shakra, A., and Zeiger, E. (1997) Formation of 8-hydroxy-2′-deoxyguanosine following treatment of 2′-deoxyguanosine or DNA by hydrogen peroxide or glutathione. *Mutat. Res. 390*, 45−50.
(13) Cadet, J., Douki, T., Gasparutto, D., and Ravanat, J. L. (2003) Oxidative damage to DNA: Formation, measurement and biochemical features. *Mutat. Res. 531*, 5−23.
(14) Wood, M. L., Dizdaroglu, M., Gajewski, E., and Essigmann, J. M. (1990) Mechanistic studies of ionizing radiation and oxidative mutagenesis: Genetic effects of a single 8-hydroxyguanine (7-hydro-8-oxoguanine) residue inserted at a unique site in a viral genome. *Biochemistry 29*, 7024−7032.
(15) Klungland, A., Rosewell, I., Hollenbach, S., Larsen, E., Daly, G., Epe, B., Seeberg, E., Lindahl, T., and Barnes, D. E. (1999) Accumulation of premutagenic DNA lesions in mice defective in removal of oxidative base damage. *Proc. Natl. Acad. Sci. U.S.A. 96*, 13300−13305.
(16) Choi, J. Y., Kim, H. S., Kang, H. K., Lee, D. W., Choi, E. M., and Chung, M. H. (1999) Thermolabile 8-hydroxyguanine DNA glycosylase with low activity in senescence accelerated mice due to a single-base mutation. *Free Radical Biol. Med. 27*, 848−854.
(17) Shibutani, S., Takeshita, M., and Grollman, A. P. (1991) Insertion of specific bases during DNA synthesis past the oxidation-damaged base 8-oxodG. *Nature 349*, 431−434.
(18) Wagner, J. R., and Cadet, J. (2010) Oxidation reactions of cytosine DNA components by hydroxyl radical and one-electron oxidants in aerated aqueous solutions. *Acc. Chem. Res. 43*, 564−571.
(19) Luo, Y., Henle, E. S., and Linn, S. (1996) Oxidative damage to DNA constituents by iron-mediated Fenton reactions. The deoxycytidine family. *J. Biol. Chem. 271*, 21167−21176.
(20) Wallace, S. S. (2002) Biological consequences of free radical-damaged DNA bases. *Free Radical Biol. Med. 33*, 1−14.
(21) Purmal, A. A., Kow, Y. W., and Wallace, S. S. (1994) Major oxidative products of cytosine, 5-hydroxycytosine and 5-hydroxyuracil, exhibit sequence context-dependent mispairing *in vitro*. *Nucleic Acids Res. 22*, 72−78.
(22) Kreutzer, D. A., and Essigmann, J. M. (1998) Oxidized, deaminated cytosines are a source of C → T transitions in vivo. *Proc. Natl. Acad. Sci. U.S.A. 95*, 3578−3582.
(23) Negishi, K., Sekine, D., Morimitsu, T., Suzuki, T., Okugawa, Y., Kawakami, A., Otsuka, C., Oyama, H., and Loakes., D. (2007) Oligonucleotide transformation for the study of mutagenic specificities of DNA lesions in yeast. *Nucleic Acids Symp. Ser. 51*, 211−212.
(24) Vaisman, A., and Woodgate, R. (2001) Unique misinsertion specificity of pol ι may decrease the mutagenic potential of deaminated cytosines. *EMBO J. 20*, 6520−6529.
(25) Zahn, K. E., Averill, A., Wallace, S. S., and Doublié, S. (2011) The miscoding potential of 5-hydroxycytosine arises due to template instability in the replicative polymerase active site. *Biochemistry 50*, 10350−10358.
(26) Eide, L., Luna, L., Gustad, E. C., Henderson, P. T., Essigmann, J. M., Demple, B., and Seeberg, E. (2001) Human endonuclease III acts preferentially on DNA damage opposite guanine residues in DNA. *Biochemistry 40*, 6653−6659.
(27) Hatahet, Z., Kow, Y. W., Purmal, A. A., Cunningham, R. P., and Wallace, S. S. (1994) New substrates for old enzymes. 5-Hydroxy-2′-deoxycytidine and 5-hydroxy-2′-deoxyuridine are substrates for *Escherichia coli* endonuclease III and formamido-pyrimidine DNA N-glycosylase, while 5-hydroxy-2′-deoxyuridine is a substrate for uracil DNA N-glycosylase. *J. Biol. Chem. 269*, 18814−18820.
(28) Tremblay, S., and Wagner, J. R. (2008) Dehydration, deamination and enzymatic repair of cytosine glycols from oxidized poly(dG-dC) and poly(dI-dC). *Nucleic Acids Res. 36*, 284−293.
(29) Thayer, M. M., Ahern, H., Xing, D., Cunningham, R. P., and Tainer, J. A. (1995) Novel DNA binding motifs in the DNA repair enzyme endonuclease III crystal structure. *EMBO J. 14*, 4108−4120.
(30) Fromme, J. C., and Verdine, G. L. (2003) Structure of a trapped endonuclease III-DNA covalent intermediate. *EMBO J. 22*, 3461−3471.
(31) Cantor, C. R., Warshow, M. M., and Shapiro, H. (1970) Oligonucleotide interactions. 3. Circular dichroism studies of the conformation of deoxyoligonucleotides. *Biopolymers 9*, 1059−1077.
(32) Marky, L. A., Blumenfeld, K. S., Kozlowski, S., and Breslauer, K. J. (1983) Salt-dependent conformational transitions in the self-complementary deoxydodecanucleotide d(CGCGAATTCGCG): Evidence for hairpin formation. *Biopolymers 22*, 1247−1257.
(33) Kaushik, M., Suehl, N., and Marky, L. A. (2007) Calorimetric unfolding of the bimolecular and i-motif complexes of the human telomere complementary strand, $d(C_3TA_2)_4$. *Biophys. Chem. 126*, 154−164.
(34) Courtenay, E. S., Capp, M. W., Anderson, C. F., and Record, M. T. Jr. (2000) Vapor pressure osmometry studies of osmolyte−protein interactions: Implications for the action of osmoprotectants in vivo and for the interpretation of "osmotic stress" experiments in vitro. *Biochemistry 39*, 4455−4471.
(35) Marky, L. A., and Breslauer, K. J. (1987) Calculating thermodynamic data for transitions of any molecularity from equilibrium melting curves. *Biopolymers 26*, 1601−1620.
(36) Rentzeperis, D., Marky, L. A., Dwyer, T. J., Geierstanger, B. H., Pelton, J. G., and Wemmer, D. E. (1995) Interaction of minor groove ligands to an AAATT/AATTT site: Correlation of thermodynamic characterization and solution structure. *Biochemistry 34*, 2937−2945.
(37) Wing, R., Drew, H., Takano, T., Broka, C., Tanaka, S., Itakura, K., and Dickerson, R. E. (1980) Crystal structure analysis of a complete turn of B-DNA. *Nature 287*, 755−758.
(38) Marky, L. A., Blumenfeld, K. S., Kozlowski, S., and Breslauer, K. J. (1983) Salt-dependent conformational transitions in the self-complementary deoxydodecanucleotide d(CGCGAATTCGCG): Evidence for hairpin formation. *Biopolymers 22*, 1247−1257.
(39) Bloomfield, V. A., Crothers, D. M., and Tinoco, I., Jr., Eds. (1999) Electronic and Vibrational Spectroscopy. *Nucleic Acids: Structures, Properties, and Functions*, pp 185−196, University Science Books, Sausalito, CA.
(40) Boelens, R., Scheek, R. M., Dijkstra, K., and Kapten, R. (1985) Sequential assignment of imino- and amino-proton resonances in ^{1}H NMR spectra of oligonucleotides by two-dimensional NMR spectroscopy. Application to a lac operator fragment. *J. Magn. Reson. 62*, 378−386.
(41) Lee, C. H., Mizusawa, H., and Kakefuda, T. (1981) Unwinding of double-stranded DNA helix by dehydration. *Proc. Natl. Acad. Sci. U.S.A. 78*, 2838−2842.
(42) Bastos, M., Castro, V., Mrevlishvili, G., and Teixeira, J. (2004) Hydration of ds-DNA and ss-DNA by neutron quasielastic scattering. *Biophys. J. 86*, 3822−3827.
(43) LaFrancois, C. J., Fujimoto, J., and Sowers, L. C. (1998) Synthesis and characterization of isotopically enriched pyrimidine deoxynucleoside oxidation damage products. *Chem. Res. Toxicol. 11*, 75−83.
(44) Suen, W., Spiro, T. G., Sowers, L. C., and Fresco, J. R. (1999) Identification by UV resonance Raman spectroscopy of an imino tautomer of 5-hydroxy-2′-deoxycytidine, a powerful base analog transition mutagen with a much higher unfavored tautomer frequency than that of the natural residue 2′-deoxycytidine. *Proc. Natl. Acad. Sci. U.S.A. 96*, 4500−4505.
(45) La Francois, C. J., Jang, Y. H., Cagin, T., Goddard, W. A. III, and Sowers, L. C. (2000) Conformation and proton configuration of pyrimidine deoxynucleoside oxidation damage products in water. *Chem. Res. Toxicol. 13*, 462−470.
(46) Young, M. A., Jayaram, B., and Beveridge, D. L. (1998) Local dielectric environment of B-DNA in solution: Results from a 14 ns molecular dynamics trajectory. *J. Phys. Chem. B 102*, 7666−7669.
(47) Thuong, N. T., and Hêlène, C. (1993) Sequence-specific recognition and modification of double-helical DNA by oligonucleotides. *Angew. Chem., Int. Ed. 32*, 666−690.
(48) Singleton, S. F., and Dervan, P. B. (1992) Influence of pH on the equilibrium association constants for oligodeoxyribonucleotide-directed triple helix formation at single DNA sites. *Biochemistry 31*, 10995−11003.

(49) Hall, R. H. (1971) in *The Modified Nucleosides in Nucleic Acids*, pp 192−194, Columbia University Press, New York.
(50) Leitner, D., Schröder, W., and Weisz, K. (2000) Influence of sequence-dependent cytosine protonation and methylation on DNA triplex stability. *Biochemistry 39*, 5886−5892.
(51) Krauss, M., and Osman, R. (1997) Electronic spectra of the H and OH adducts of cytosine. *J. Phys. Chem. A 101*, 4117−4120.
(52) Cysewski, P. (1999) Structure and properties of hydroxyl radical modified nucleic acid components: Tautomerism and miscoding propoerties of 5-hydroxycytosine. *THEOCHEM 466*, 49−58.
(53) Czerminski, R., Lesyng, B., and Pohorille, A. (1979) Tautomerism of pyrimidine bases-uracil, cytosine, isocytosine: Theoretical study with complete optimization of geometry. *Int. J. Quantum Chem. 16*, 605−613.
(54) Peyret, N., Seneviratne, P. A., Allawi, H. T., and SantaLucia, J. Jr. (1999) Nearest-neighbor thermodynamics and NMR of DNA sequences with internal A·A, C·C, G·G, and T·T mismatches. *Biochemistry 38*, 3468−3477.
(55) Singh, S. K., Szulik, M. W., Ganguly, M., Khutsishvili, I., Stone, M. P., Marky, L. A., and Gold, B. (2011) Characterization of DNA with an 8-oxoguanine modification. *Nucleic Acids Res. 39*, 6789−6801.
(56) Lipscomb, L .A., Peek, M. E., Morningstar, M. L., Verghis, S. M., Miller, E. M., Rich, A., Essigmann, J. M., and Williams, L. D. (1995) X-ray structure of a DNA 5′-d(CGC-oxoG-AATTCGCG) decamer containing 7,8-dihydro-8-oxoguanine. *Proc. Natl. Acad. Sci. U.S.A. 92*, 719−723.
(57) Oda, Y., Uesugi, S., Ikehara, M., Nishimura, S., Kawase, Y., Ishikawa, H., Inoue, H., and Ohtsuka, E. (1991) NMR studies of a DNA containing 8-hydroxydeoxyguanosine. *Nucleic Acids Res. 19*, 1407−1412.
(58) Ganguly, M., Wang, R.-W., Marky, L. A., and Gold, B. (2010) Thermodynamic characterization of DNA with 3-deazaadenine and 3-methyl-3-deazaadenine substitutions. *J. Phys. Chem. B 114*, 7656−7661.
(59) Ganguly, G., Wang, F., Kaushik, M., Stone, M. P., Marky, L. A., and Gold, B. (2007) A study of 7-deaza-2′-deoxyguanosine·2′-deoxycytidine base pairing in DNA. *Nucleic Acids Res. 35*, 6181−6195.
(60) Kowal, E., Ganguly, M., Pallan, P., Marky, L. A., Gold, B., Egli, M., and Stone, M. P. (2011) Altering the electrostatic potential in the major groove: Thermodynamic and structural characterization of 7-deaza-2′-deoxyadenosine·dT base pairing in DNA. *J. Phys. Chem. B 115*, 13925−13934.
(61) Plum, G. E., and Breslauer, K. J. (1994) DNA lesions. A thermodynamic perspective. *Ann. N.Y. Acad. Sci. 726*, 45−55.
(62) Mol, C. D., Parikh, S. S., Putnam, C. D., Lo, T. P., and Tainer, J. A. (1999) DNA repair mechanisms for the recognition and removal of damaged DNA bases. *Annu. Rev. Biophys. Biomol. Struct. 28*, 101−128.
(63) Biswas, T., Clos, L. J. II, SantaLucia, J. Jr., Mitra, S., and Roy, R. (2002) Binding of specific DNA base-pair mismatches by N-methylpurine-DNA glycosylase and its implication in initial damage recognition. *J. Mol. Biol. 320*, 503−513.
(64) O'Brien, P. J., and Ellenberger, T. (2004) Dissecting the broad substrate specificity of human 3-methyladenine-DNA glycosylase. *J. Biol. Chem. 279*, 9750−9757.
(65) Wolfe, A. E., and O'Brien, P. J. (2009) Kinetic mechanism for the flipping and excision of 1,N6-ethenoadenine by human alkyladenine DNA glycosylase. *Biochemistry 48*, 11357−11369.
(66) Rubinson, E. H., Gowda, A. S. P., Spratt, T. E., Gold, B., and Eichman, B. F. (2010) An unprecedented nucleic acid capture mechanism for excision of DNA damage. *Nature 468*, 406−411.
(67) Fujii, T., Saito, T., and Nakasaka, T. (1989) Purines. XXXIV. 3-Methyladenosine and 3-methyl-2′-deoxyadenosine: Their synthesis, glycosidic hydrolysis, and ring fission. *Chem. Pharm. Bull. 37*, 2601−2609.